

# Compatibilities for Boundary Extraction

Josef Pauli and Gerald Sommer

Christian-Albrechts-Universität zu Kiel,  
Institut für Informatik und Praktische Mathematik,  
Preußerstraße 1-9, D-24105 Kiel,  
[www.ks.informatik.uni-kiel.de/~jpa{~gs}](http://www.ks.informatik.uni-kiel.de/~jpa{~gs}),  
[jpa{gs}@ks.informatik.uni-kiel.de](mailto:jpa{gs}@ks.informatik.uni-kiel.de)

**Abstract.** The work presents a methodology contributing to boundary extraction in images of approximate polyhedral objects. We make extensive use of basic principles underlying the process of image formation and thus reduce the role of object-specific knowledge. Simple configurations of line segments are extracted subject to geometric-photometric compatibilities. The perceptual organization into polygonal arrangements is based on geometric regularity compatibilities under projective transformation. The combination of several compatibilities yields a saliency function for extracting a list of most salient structures. Based on systematic measurements during an experimentation phase the adequacy and degrees of compatibilities are determined. The methodology is demonstrated for technical objects of electrical scrap located in cluttered scenes.

## 1 Introduction

Computer Vision procedures are based on expectations whose spectrum stretches from general assumptions, e.g. ramp profiles of gray-value edges, to specific models for object recognition, e.g. relational structures of geometric entities. *Which expectations can be applied reasonably along the chain of processing and how are they acquired ?* This question is confronted with the *variance/bias dilemma*. If expectations are too general then the number of possible interpretations of image contents will increase dramatically. Otherwise, if expectations are too specific and do not comply with the variability of possible situations then relevant structures can hardly be detected. We propose a methodology of treating the dilemma for the task of boundary extraction. The characteristics are the following.

First, the theoretical concept of *invariance* (well-established in Computer Vision [9, pp. 95-160]) is relaxed into the practical concept of *compatibility*. The use of compatibilities reduces the amount of object-specific knowledge for medium-level vision tasks like attention control and *boundary extraction*. Second, we maximally exploit those kind of compatibilities which originate and are inherent in the *three-dimensional nature* of objects and in the *image formation principles*. Compatibilities between geometric and photometric features and between elementary and structured geometric entities are considered. The related work in [10] uses *geometric quasi-invariants* for curved objects, but doesn't treat the gap between geometry and photometry. Third, the compatibilities are determined on the basis of *statistical measurements* which must be taken during

an *experimentation phase* prior to application (importance repeatedly stressed in [3]). Systematic experiments are needed for *quality assessment* and *threshold setting* of procedures of line extraction and perceptual grouping. Fourth, we integrate a series of gestaltic cues spanning over *signal level*, *primitive level*, *structural level*, and *assembly level* (four-level classification proposed in [5]).

We present a catalogue of propositions each describing a compatibility. They depend on thresholds  $\delta_i$  which must be determined in an experimentation phase.

## 2 Geometric-photometric compatibilities

The propositions in this section describe compatibilities between global geometric entities and local gray-value structures in the image.

### 2.1 Orientation compatibility between lines and edges

The *orientation-deviation* between orientation  $\phi$  of an object boundary line in the image (assuming polar form representation) and the orientations  $\mathcal{I}^O(p_i)$  of all gray-value edges along the points  $(p_1, \dots, p_N)$  of a segment  $\mathcal{L}$  of the image line is defined by

$$D_{LE}(\phi, \mathcal{L}) := \frac{1}{N} \cdot \sum_{i=1}^N D_{OL}(\phi, \mathcal{I}^O(p_i)) \quad (1)$$

$$D_{OL}(\phi, \mathcal{I}^O(p_i)) := \frac{\min\{|\phi - \mathcal{I}^O(p_i)|, |\phi - \mathcal{I}^O(p_i) + 180^\circ|, |\phi - \mathcal{I}^O(p_i) - 180^\circ|\}}{90^\circ} \quad (2)$$

**Proposition 1.** *Given  $\delta_1$  as permissible orientation-deviation. The line-edge orientation compatibility holds subject to image formation if  $D_{LE}(\phi, \mathcal{L}) \leq \delta_1$ .*

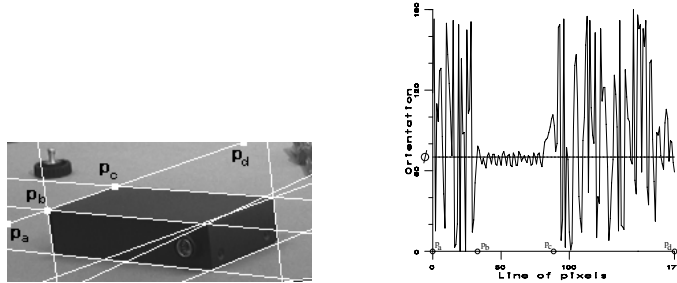


**Fig. 1.** (Left) Black box, boundary lines. (Right) Edge orientations along a line.

Figure 1 (left) shows a black box and candidate boundary lines which have been extracted by Hough transformation. For one of them, going through points  $\{p_a, p_b, p_c, p_d\}$ , we show the course of edge orientations (right), which are the local gradient angles. In consensus with Proposition 1, just for the boundary segment  $(p_b, \dots, p_c)$  the course is close to the line orientation.

## 2.2 Junction compatibility between pencils and corners

A *pencil* is a simple configuration of  $M$  line segments meeting at one common *pencil point* [1, pp. 8,17]. At the gray-level corner located nearest to a pencil point the two-dimensional gray-value structure will be considered. The *junction-deviation* between a pencil at pencil point  $p_l$  with line orientations  $\mathcal{A} := (\alpha_1, \dots, \alpha_M)$  and a collection of edge sequences meeting at corner point  $p_c$  with local orientations  $\mathcal{B} := (\beta_1, \dots, \beta_M)$  is defined by

$$D_{PC}(p_l, p_c, \mathcal{A}, \mathcal{B}) := \omega_1 \cdot D_{JP}(p_l, p_c) + \omega_2 \cdot D_{JO}(\mathcal{A}, \mathcal{B}) \quad (3)$$

$$D_{JP}(p_l, p_c) := \frac{\|p_l - p_c\|}{I_d} \quad (4)$$

$$D_{JO}(\mathcal{A}, \mathcal{B}) := \frac{1}{180^\circ \cdot M} \cdot \sum_{i=1}^M \min\{|\alpha_i - \beta_i|, |\alpha_i - \beta_i + 360^\circ|, |\alpha_i - \beta_i - 360^\circ|\} \quad (5)$$

It is a weighted summation of two components, i.e. the Euclidean distance between pencil point and corner point (normalized by the constant diagonal  $I_d$  of a standard image size, e.g.  $512 \times 512$  pixel), and the deviation between the orientation of a pencil line and of a corresponding edge sequence (averaged over all such pairs).

**Proposition 2.** *Given  $\delta_2$  as permissible junction-deviation. The pencil-corner junction compatibility holds subject to image formation if  $D_{PC}(p_l, p_c, \mathcal{A}, \mathcal{B}) \leq \delta_2$ .*

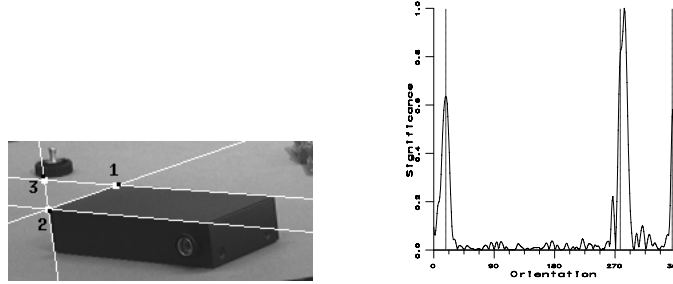


**Fig. 2.** (Left) Subset of boundary lines, pencil points, corner points. (Right) Orientation-dependent significance measurements for edge sequences at point 2.

Figure 2 (left) shows a subset of four boundary lines, three pencil points (white squares) with indices 1,2,3, and a subset of three nearest gray-value corner points (black squares). The latter are extracted by the SUSAN operator [7]. For example, the pencil-corner junction compatibility holds for point 2, where we have a pencil of three lines. The diagram on the right shows the characterization of the local gray-value structure, i.e. orientation-dependent significance measurement for the occurrence of edge sequences, which is computed by a steerable wedge filter [6]. The three peaks, which indicate the occurrence of three edge sequences for certain orientations, are close to three vertical diagram lines, which indicate the orientations of the pencil lines. This kind of compatibility holds as well for point 1 but not for point 3 (not shown in the right diagram).

### 2.3 Phase compatibility between parallels and ramps

The *local phase* characterizes the type of gray-value edges, i.e. ascending or descending ramps, and top or bottom directed roofs [2, pp. 258-278]. Being a one-dimensional concept, we show the phase behavior exemplary by scanning the virtual, vertical line in Figure 3 (left) from top to bottom. At the first and second intersection points with the object boundary the ramps are descending, and at the third point the ramp is ascending. This behavior is in consensus with the quantitative course of the polar angle (representing the local phases), as shown on the right. In particular, the sign of the local phase at the first boundary line is converse to the sign at the opposite boundary line of the object. Generally, this is true if all gray values of the object are lower or higher than the gray values of the local background. Based on this observation and assumption, a criterion for the detection of opposite boundary lines of an object is proposed.

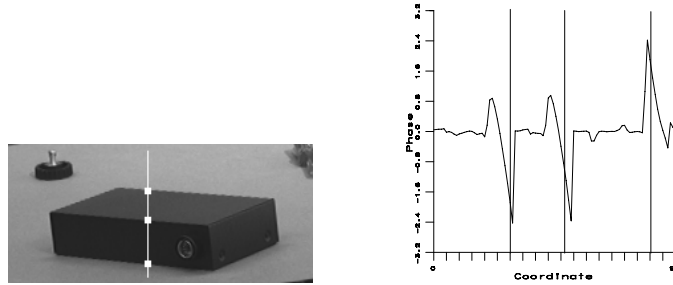


**Fig. 3.** (Left) Virtual line. (Right) Local phases along the line.

Let  $\mathcal{L}_1$  and  $\mathcal{L}_2$  be two approximate parallel line segments. The two mean values of the local phases along these segments (computed orthogonal to the line orientations) are denoted by  $f^{ph}(\mathcal{L}_1)$  and  $f^{ph}(\mathcal{L}_2)$ . We define the *phase-similarity* between the two mean phases such that the similarity between equal phases is 1 and the similarity between phases with converse signs is 0.

$$D_{PR}(\mathcal{L}_1, \mathcal{L}_2) := \left| 1 - \frac{|f^{ph}(\mathcal{L}_1) - f^{ph}(\mathcal{L}_2)|}{\pi} \right| \quad (6)$$

**Proposition 3.** *Given  $\delta_3$  as permissible deviation from 0. The parallel-ramp phase compatibility holds subject to image formation if  $D_{PR}(\mathcal{L}_1, \mathcal{L}_2) \leq \delta_3$ .*

The presented geometric-photometric compatibilities are the foundation for applying the following list of pure geometric compatibilities.

### 3 Geometric compatibilities for perceptual organization

The propositions in this section describe compatibilities between elementary and structured geometric entities which are subject to the process of image formation, i.e. approximate perspective transformation.

### 3.1 Patterns of Hough peaks for approximate-parallel lines

Based on polar parameters  $r$  and  $\phi$  of straight lines we apply *Hough transformation* for line extraction. The horizontal and vertical axes of the Hough image are taken correspondingly. The Hough transformation of parallel image lines (having identical value  $\phi$ ) yields a horizontal sequence of peaks in the Hough image. Under projective transformation, two parallel lines in 3D remain almost parallel in the image, i.e. there is a small *angle-deviation*  $D_{OL}(\phi_1, \phi_2)$ .

**Proposition 4.** *Given  $\delta_4$  as permissible angle-deviation. The parallelism compatibility of two lines holds subject to image formation if  $D_{OL}(\phi_1, \phi_2) \leq \delta_4$ .*

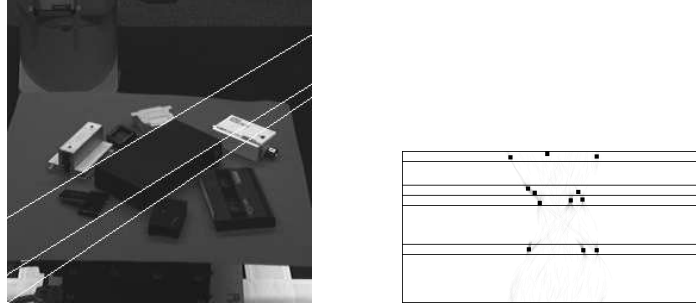


**Fig. 4.** (Left) Subset of three approximate parallel boundary lines for the black box object. (Right) Hough image and peaks marked by black squares.

Considering Proposition 4, parallel 3D lines occur as peaks in the Hough image located within a horizontal stripe of height  $\delta_4$  (In Subsection 3.3, the vanishing-point compatibility introduces further constraints). Figure 4 shows the Hough image on the right when applying Hough transformation to the image on the left. We restricted the process to a quadrangle image window around the black box and selected 12 peaks which are organized in four stripes of three peaks, respectively. For example, three *approximate parallel lines* are shown on the left, which are specified by the peaks in the third stripe of the Hough image.

### 3.2 Regularity compatibilities for polygons

Approximate parallel line segments may occur in *approximate regular polygons*. The basic component for describing polygon regularities is a *polyline*. We specify a polygon as the union of two non-overlapping polylines  $\mathcal{G}_1$  and  $\mathcal{G}_2$ , possibly including single line segments located at the end of each polyline, respectively. Figure 5 shows two regular polygons, the left one contains a pair of reflected polylines, the right one a pair of parallel polylines. The angle-deviation  $D_{OP}(\mathcal{G}_1, \mathcal{G}_2)$  between two approximate parallel polylines is defined as the mean value of angle-deviations between the constituting approximate parallel line segments.

**Proposition 5.** *Given  $\delta_5$  as permissible angle-deviation. The parallelism compatibility of two polylines holds subject to image formation if  $D_{OP}(\mathcal{G}_1, \mathcal{G}_2) \leq \delta_5$ .*

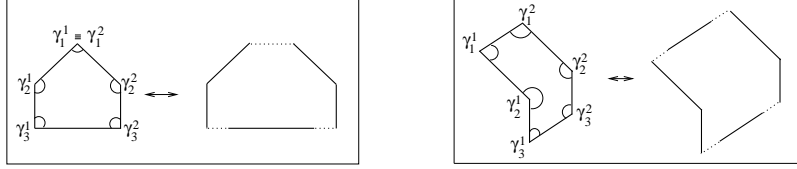


**Fig. 5.** Examples of regular polygons.

Similar propositions can be formulated for *reflection compatibility* and *right-angle compatibility*. They are based on permissible deviations from exact reflections or exact right-angles, respectively.

### 3.3 Vanishing-point compatibility of boundary lines

The projective transformation of parallel boundary lines yields image lines whose extensions should meet in one vanishing-point (see Figure 6). This imposes certain qualitative constraints on the courses of Hough peaks within a horizontal stripe, which we summarize as the *vanishing-point compatibility*. A similar constraint was formulated in [8] but under slope/intercept parameterization of lines.

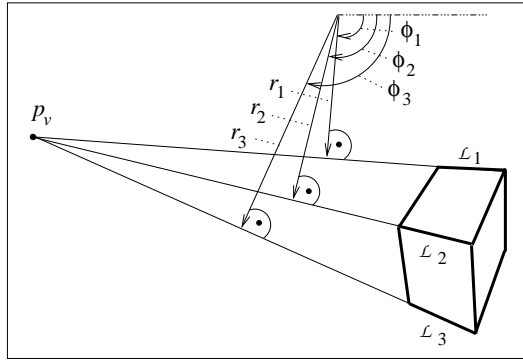


**Fig. 6.** Projected parallelepiped, van. point.

**Proposition 6.** Let  $\{\mathcal{L}_1, \dots, \mathcal{L}_V\}$  be a set of approximate parallel line segments in the image, which originate from projective transformation of parallel line segments of the 3D object boundary. The extensions of the image line segments meet at a common vanishing point  $p_v$  and can be sorted according to the strong monotony  $r_1 < \dots < r_i < \dots < r_V$  of the parameter  $r$ . For this arrangement there is a weak monotony of the angle parameter,

$$\phi_1 \geq \dots \phi_i \geq \dots \geq \phi_V \quad \text{or} \quad \phi_1 \leq \dots \phi_i \leq \dots \leq \phi_V \quad (7)$$

The vanishing-point compatibility can be examined for the Hough image in Figure 4 (right). Proposition 6 holds for the third and fourth stripe but not for the first and second stripe. To make it completely valid, we must apply a strategy which slightly modifies parameters  $r$  and  $\phi$  of the relevant image lines.

### 3.4 Pencil compatibility of meeting boundary lines

The most prominent corner type of man-made objects is a pencil of three lines. For a subset of corners all three boundary lines are visible. In the case that these image lines are extracted, we can impose the following *pencil compatibility*.

**Proposition 7.** *Let us assume a 3D pencil and the pencil point of three meeting boundary lines of an approximate polyhedral object. The projective transformation of the 3D pencil must yield just one pencil in the image plane, i.e. just one 2D pencil point.*

For example, Figure 2 (left) shows three lines intersecting at point 2. Actually, according to Proposition 7 just one intersection point is accepted which must be considered in the process of line extraction.

## 4 Experiments on boundary extraction

The presented compatibilities are the foundation for several mechanisms which make up our procedure for boundary extraction. The approach is general in the sense that an application-dependent combination can be configured by weighting the compatibilities individually. Prior to the applications, the thresholds  $\delta_i$  are determined in an experimentation phase.

Figure 7 shows some results of extracted boundaries which originate from objects located within complex environments. The procedures look for certain geometric shapes in the images by taking certain compatibilities into account. No other object-specific knowledge has been applied for boundary extraction. The left image shows the interior of a computer containing an electronic board which is of approximate rectangular shape. A small set of most salient, approximate rectangles is shown including the relevant boundary of the board. The middle image shows again the interior of a computer containing an electronic board which is of approximate, right-angled, hexagonal shape. The procedure extracted the relevant boundary as the most salient, approximate hexagon. The right image shows a set of 3D objects including the black box (see previous figures), which is of approximate, right-angled, parallelepiped shape. The relevant arrangement of polygons has been extracted in spite of complex background and low gray-value contrast between neighboring faces of the object.

By applying verified compatibilities instead of object-specific knowledge, the procedures extracted reasonable boundaries (despite of complex shape and background, and low face contrast). The boundaries can be used subsequently in strategies of visual attention, e.g. for the purpose of local object recognition.

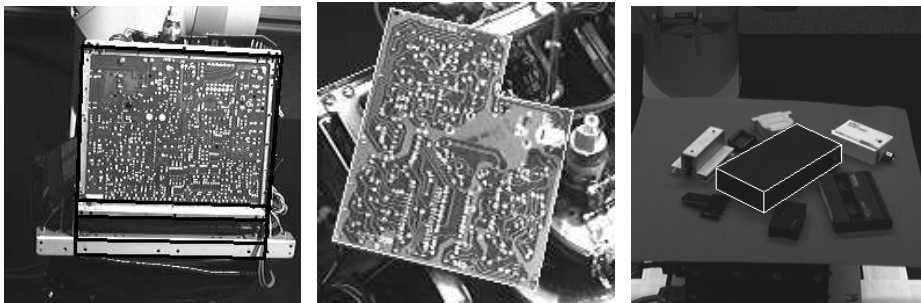


Fig. 7. Examples of extracted object boundaries.

## 5 Summary

The novelty of our methodology is that we maximally apply compatibilities for extracting necessary information from images. Compatibilities are degradations of invariants and are based on the actual effects of image formation. For the task of boundary extraction it is convenient to consider compatibilities between global geometric entities and local gray-value features, as well as compatibilities between elementary and structured geometric entities.

On the basis of systematic measurements during an experimentation phase one *approximates* the performance of certain procedures statistically and determines *degrees of compatibilities* thereof. For example, estimation errors concerning the orientation of gray-value edges can be approximated by a Gaussian. The Gaussian support is used to define threshold parameter  $\delta_1$ , which quantifies the orientation compatibility between lines and gray-value edges (see Proposition 1).

The experimentally acquired compatibilities are regarded as a compromise of the variance/bias dilemma which is inherent in the design of Computer Vision procedures. In our opinion, there is no way to determine desired levels of performance with certainty, however, systematic application-relevant experiments constitute the best foundation for the development of robust systems.

For a detailed description of our mechanisms for boundary extraction and the mechanisms of determining threshold parameters, the interested reader is referred to [4].

## References

1. O. Faugeras. *Three-Dimensional Computer Vision*. The MIT Press, Cambridge, Massachusetts, 1993.
2. G. Granlund and H. Knutsson. *Signal Processing for Computer Vision*. Kluwer Academic Publishers, Dordrecht, The Netherlands, 1995.
3. R. Haralick, R. Klette, S. Stiehl, and M. Viergever. Evaluation and validation of Computer Vision algorithms. Technical Report Number 204, Seminar Number 98101, Schloß Dagstuhl Seminars, 1998.
4. J. Pauli. Development of autonomous camera-equipped robot systems. Technical Report Number 9904, Christian-Albrechts-Universität zu Kiel, Institut für Informatik und Praktische Mathematik, 2000.
5. S. Sarkar and K. Boyer. Perceptual organization in Computer Vision – A review and a proposal for a classificatory structure. *IEEE Transactions on Systems, Man, and Cybernetics*, 23:382–399, 1993.
6. E. Simoncelli and H. Farid. Steerable wedge filters for local orientation analysis. *IEEE Transactions on Image Processing*, 5:1377–1382, 1996.
7. S. Smith and J. Brady. SUSAN – A new approach to low level image processing. *International Journal of Computer Vision*, 23:45–78, 1997.
8. T. Stahs and F. Wahl. Recognition of polyhedral objects under perspective views. *Computers and Artificial Intelligence*, 11:155–172, 1992.
9. H. Wechsler. *Computational Vision*. Academic Press, San Diego, 1990.
10. M. Zerroug and R. Nevatia. Quasi-invariant properties and 3D shape recovery of non-straight, non-constant generalized cylinders. In *Image Understanding Workshop*, pages 725–735, 1993.